RSC Advances

PAPER

Cite this: *RSC Adv.*, 2014, **4**, 34674

Ag_3PO_4 sunlight-induced photocatalyst for degradation of phenol

Thiago L. R. Hewer,*[ab] Bárbara C. Machado,[b] Renato S. Freire[a] and Roberto Guardani[b]

Received 12th May 2014
Accepted 30th July 2014

DOI: 10.1039/c4ra04457f

www.rsc.org/advances

Micrometric particles of Ag_3PO_4 were prepared by a simple precipitation method, and the as-prepared material was characterized by X-ray diffraction (XRD), field-emission scanning electron microscopy (FEG-SEM), nitrogen sorption isotherms, Raman spectroscopy and UV-visible diffuse reflectance spectrophotometry. Ag_3PO_4 particles showed excellent catalytic activity for degradation of phenol using simulated sunlight irradiation (Xenon lamp). After one hour of treatment, approximately 75% of phenol was completely mineralized. Additional experiments were conducted in order to evaluate the influence of dissolved oxygen in the photocatalytic process. During photodegradation assisted by Ag_3PO_4, it was considered that oxygen production and phenol oxidation were competitive processes.

1. Introduction

Heterogeneous photocatalysis is an efficient technology for the degradation of organic contaminants, either in aqueous media or in the gas phase. The possibility to use light as an excitation source makes this technology friendlier to the environment. The process can operate under relatively mild conditions and without the use of additional chemicals, besides catalyst. The effectiveness of the heterogeneous photocatalysis is due to its ability to produce highly reactive oxygen species such as hydroxyl radicals ($^{\bullet}OH$) and superoxide radical anion ($O_2^{\bullet -}$).[1,2] These reactive radicals are the key species in the oxidation of various organic compounds, since they are powerful oxidants, short lived and non-selective reagents.[3,4]

TiO_2 is a well known photocatalyst, due to its electronic structure, chemical stability and low cost. An important property of this catalyst is its capability to produce radical species in aqueous solution. When the semiconductor particles are excited by light with sufficient energy ($h\nu \geq E_{bg}$; $E_{bg} = 3.23$ eV for anatase), an electron–hole pair (e_{cb}^-/h_{vb}^+) is formed.[5] The photogenerated e_{cb}^-/h_{vb}^+ pairs in the semiconductor, when in contact with O_2 or H_2O and HO^- adsorbed in its surface, can lead to the formation of radical species. However, one important disadvantage of TiO_2 as a photocatalyst is its high band gap energy, which means that it is mainly excited by radiation with wavelength smaller than *ca.* 380 nm, corresponding to the UV region, which is a small fraction of the solar spectrum.[6] From the technological point of view, however, an important factor that increase the attractiveness of heterogeneous photocatalysis processes is the development of active catalysts under visible light, so that sunlight can be efficiently used as a light source.

Thus, the development of new photocatalyst materials with desirable band structure and high activity in the visible light range is still a challenge.

Recently, it has been shown that silver orthophosphate has a significant photocatalytic efficiency under visible light irradiation. This evidence is based on its performance in O_2 gas production from water splitting, and the strong oxidation power in methylene blue degradation studied by Withers.[7] After this landmark article, Ag_3PO_4 photocatalytic properties have been evaluated in terms of the performance in organic pollutants degradation, such as dyes in aqueous solution.[8,9] In particular, recent studies focus on the synthesis of silver orthophosphate semiconductor with specific particle morphology, surface structure and size distribution.[10–12]

In the present study, micrometric Ag_3PO_4 particles were prepared by a simple precipitation method and characterized. The photocatalytic activity of the material was evaluated by phenol degradation under different conditions. The photocatalytic activity of the silver orthophosphate was compared with TiO_2 P25 catalyst under Xe lamp irradiation. Furthermore, the role of dissolved oxygen in the degradation process by both semiconductors is discussed.

2. Experimental

2.1 Ag_3PO_4 preparation

Silver orthophosphate materials were prepared by the conventional ion exchange/precipitation method. $AgNO_3$ and Na_3PO_4 aqueous solutions were prepared with 0.2 and 0.24 mol L^{-1}, respectively. Using a peristaltic pump and flow rate of 5 mL min^{-1}, 43 mL of Na_3PO_4 solution were pumped into 107 mL of $AgNO_3$ solution. After complete transfer, the mixture was kept

[a]*University of São Paulo, Institute of Chemistry, CEP 05508-000, São Paulo, Brazil. E-mail: hewer@iq.usp.br; Fax: +55 11 3091 1495; Tel: +55 11 3091 1495*

[b]*University of São Paulo, Department of Chemical Engineering-POLI, CEP 05508-900, São Paulo, Brazil*

under stirring during 5 h at room temperature. The silver orthophosphate was dialyzed in a 2500 kDa semipermeable cellulose membrane. Finally, the material was filtered and dried at 80 °C in a stove. The TiO_2 P25 (anatase and rutile) was used as received from Evonic.

2.2 Photocatalyst characterization

Materials were examined by scanning electron microscopy (SEM) performed with a FEG-SEM (JSM-7410, Jeol), operated at an acceleration voltage of 2.0 kV with secondary electron detector. A few droplets of a sample suspended in isopropyl alcohol were placed on a carbon adhesive and dried under vacuum at 70 °C for 12 hours and then analyzed in the microscope. Nitrogen sorption isotherms were conducted at −196 °C using a volumetric adsorption analyzer (Quantachrome, Model 100E). Surface area was determined according to the standard Brunauer, Emmet and Teller (BET) method.[13] Powder X-ray diffraction (XRD) patterns were recorded on a Miniflex X-ray diffractometer (Rigaku) equipped with Cu tube ($\lambda = 1.5418$ Å). Data were collected at 30 kV, 15 mA, in the range between $4^\circ \leq 2\theta \leq 90^\circ$ with step size of 0.02° and a count time of 2 s per step. Raman spectra were recorded in a Renishaw Raman spectroscope with 633 nm laser excitation.

2.3 Evaluation of the photocatalytic activity of the materials

Experiments were performed in an open batch system. Treatments were conducted using a 400 cm^3 cylindrical glass reactor equipped with a magnetic stirrer (stirring rate: 500 rpm), sintered glass disperser and water cooling jacket (temperature: 23 °C).

The photocatalytic evaluation was performed using 320 mL of 50 mg L^{-1} phenol aqueous solutions and 320 mg of Ag_3PO_4 or TiO_2 P25 (Evonic) suspended particles. The suspension was kept in the dark for 20 minutes. A 35 W xenon lamp (MaxiXenon, model 10000K) was employed as simulated sunlight source (emission in UVA and visible regions). After this adsorption step the suspension was irradiated during 300 minutes. At convenient intervals, samples were removed from the reactor and filtered through a 0.20 μm PTFE membrane filter. The supernatant was separated and analyzed. Some catalytic experiments were performed bubbling pure oxygen (15 L h^{-1}) into the phenol solutions during the treatment.

The phenol concentration was monitored by high-performance liquid chromatography (Shimadzu, LC 20AT HPLC) equipped with a GL-7450 UV-Vis detector (Shimadzu) and a Shim-pack separation column (Shimadzu, XR-ODS). Elution was monitored at 270 nm. The mobile phase was a mixture of methanol and acetic acid water solution (80/20, v/v). Mineralization was evaluated by monitoring total organic carbon (Shimadzu 5000A TOC analyzer). The concentration of dissolved oxygen in water was measured on-line using O_2 electrodes (YSI inc., Model 55). Generation of hydroxyl radical was investigated using the photoluminescence (PL) method with coumarin as a chemical probe.[14] These experiments were performed similar to the photodegradation experiments. After irradiation, with excitation radiation at 332 nm, the PL intensity of 7-hydroxycoumarin generated was measured (HITACHI, Model F-4500).

3. Results and discussion

The morphology of the as-prepared Ag_3PO_4 was observed by field emission scanning electron microscopy. FEG-SEM images (Fig. 1a and b) show particles with a polyhedral morphology similar to rhombic dodecahedral particles. As shown in Fig. 1c, the preparation method leads to a homogeneous and narrow particle size distribution, with mean particle size of approximately 2.2 ± 0.4 micrometers. Moreover, the micrometric particles apparently have a smooth surface (Fig. 1b).

The textural characterization was made by nitrogen sorption isotherms. Fig. 2a shows isotherms for the Ag_3PO_4 particles. According to IUPAC, Ag_3PO_4 particles have a type VI adsorption isotherm, which corresponds to non-porous and smooth surface materials.[15] The stepwise change in the isotherm corresponds to the multilayer of N_2 molecules adsorption on uniform particles surface. The surface area was obtained by BET method in the adsorption branch.[13]

For Ag_3PO_4 micrometric materials, the specific surface area was estimated as 18 m^2 g^{-1}. The crystallographic structure of the Ag_3PO_4 particles was determined by X-ray powder diffractometry (XRD), as shown in Fig. 2b. The XRD pattern indicates that the material has a body-centered cubic (b.c.c, lattice) crystalline structure. This structure consists of regular tetrahedric phosphate ions forming a b.c.c lattice with six Ag^+ ions occupying one half of the twelve sites of two-fold symmetry present in the crystalline structure and is typical for silver orthophosphate.[16]

The photocatalytic activity of semiconductors under visible and UV light irradiation is an imperative parameter to improve the applicability of the photocatalysts in the treatment of different pollutants. Fig. 3 shows the optical characteristics of

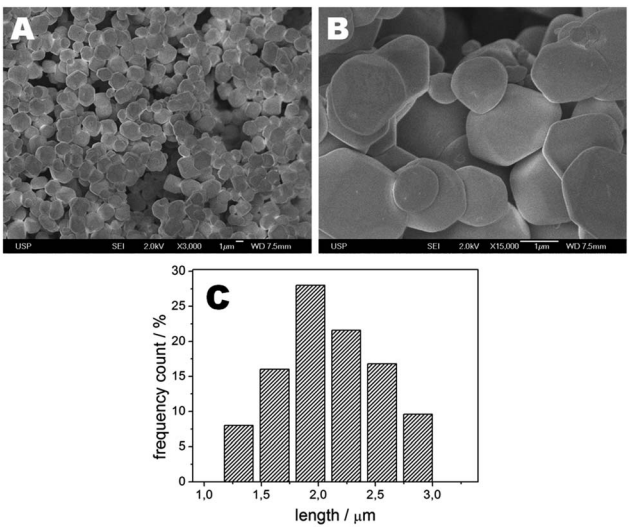

Fig. 1 Scanning electron microscopy (SEM) images of the Ag_3PO_4 photocatalyst particles. (A) low magnification; (B) high magnification. (C) particles size distribution histogram.

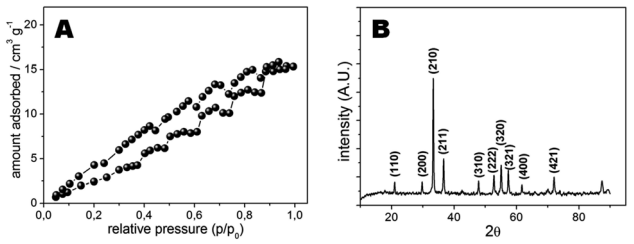

Fig. 2 Structural and textural characterization of the Ag_3PO_4 particles. (A) Nitrogen sorption isotherms; (B) X-ray diffraction analysis (XRD).

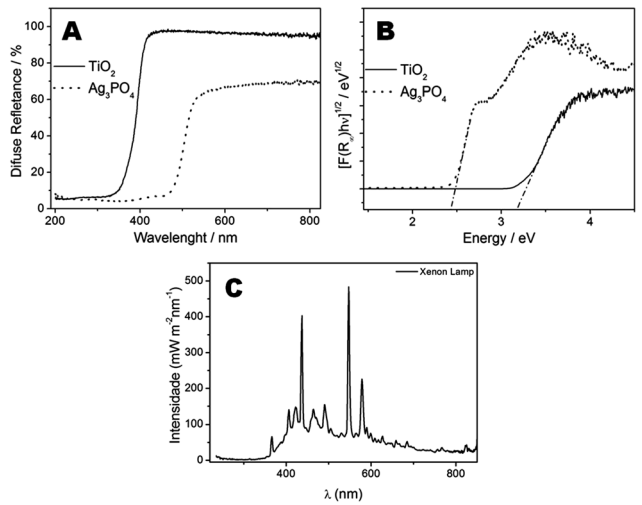

Fig. 3 Light absorption characteristics of Ag_3PO_4 and TiO_2 (P25) particles. (A) UV-Vis diffuse reflectance spectra; (B) Kubelca-Munk function ($F(R_D)$). (C) Xe lamp light emission spectrum.

Ag_3PO_4 samples based on diffuse reflectance spectra. As shown in Fig. 3a, the range of most intense light absorption of the Ag_3PO_4 particles was observed for wavelengths smaller than approximately 510 nm. The TiO_2 P25, by far the most common catalyst used in photocatalysis, has a range of more intense absorption for wavelengths smaller than 390 nm. The differences in radiation absorption range between these two materials have a direct relation with their band-gap energies. Using the Kubelka-Mulk function it was possible to evaluate the band-gap energy of both photocatalysts (Fig. 3b).[17] As expected, the optical band gap of TiO_2 P25 was 3.23 eV,[18] and the optical band gap for Ag_3PO_4 was 2.45, which is in agreement with its visible light absorption capacity.[7,19] Thus, the Ag_3PO_4 particles exhibit light absorption in the UV-Vis region, a favorable property in terms of application in photo-oxidation processes, since a small fraction (4%) of solar radiation is in the UV region, while visible light is far more abundant (46%).[20,21] Thus, Ag_3PO_4 could utilize more efficiently solar energy as irradiation source. Fig. 3c shows emission spectrum of the Xe lamp employed during the photocatalytic experiments, these UV-Vis light conditions are similar to that observed in solar radiations.[20,21] Obviously, using this radiation source, more photons will be available to excite the Ag_3PO_4 compared to those capable of exciting TiO_2. The semiconductor excitation is the *sine qua non* point in photocatalysis. However, others factors like particle morphology, superficial properties, surface area, e_{cb}^-/h_{vb}^+ recombination and presence of the electron scavengers also are very important for this heterogeneous processes.

3.1 Photocatalytic activity

The photocatalytic activity of Ag_3PO_4 particles using simulated sunlight irradiation was evaluated for phenol degradation. Fig. 4 shows phenol photodegradation and mineralization results obtained with TiO_2 and Ag_3PO_4 catalysts, under artificial light source and oxygenated media. TiO_2 and Ag_3PO_4 showed very similar performances in these conditions. After 180 minutes of treatment, practically all the phenol was degraded using both catalysts. However, complete mineralization of phenol was reached after 300 minutes of treatment using TiO_2 as photocatalyst. In the same treatment time, Ag_3PO_4 catalyst allowed approximately 80% of phenol mineralization. Complete degradation was achieved after 150 minutes of treatment. This behavior was not observed when the photodegradation was investigated without oxygen bubbling in the solution (Fig. 5).

The TiO_2 efficiency was strongly influenced by the limitation of dissolved oxygen concentration in the solution. Without O_2 bubbling in the system, no more than 35% of phenol degradation was obtained using TiO_2, and approximately 30% of TOC decrease was achieved in 180 minutes of reaction time. By comparing these results with those obtained with oxygen bubbling (Fig. 4), the observed decrease in the TiO_2 efficiency can be roughly estimated as 2.5 times for 180 minutes of reaction.

On the other hand, the results of experiments with Ag_3PO_4 particles indicate that oxygen bubbling apparently did not affect the phenol degradation efficiency, as can be observed by comparing Fig. 4 and 5. In fact, an improvement in degradation efficiency was observed, since complete phenol degradation was observed in 120 minutes of treatment in the absence of O_2 bubbling, compared with *ca.* 85% degradation with O_2 bubbling system. When the TiO_2 and Ag_3PO_4 photocatalytic performances were compared for experiments conducted under the most favourable conditions for each catalyst, namely with and without oxygen bubbling, respectively, phenol oxidation efficiencies for these two catalysts were close. However, if particles surface areas of the materials are taken into account in this

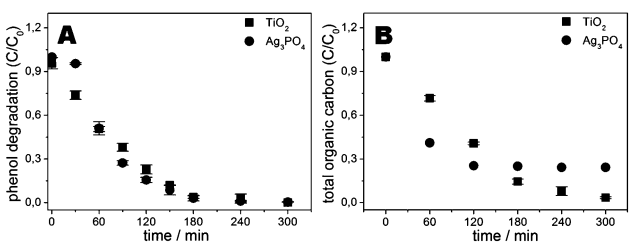

Fig. 4 Photocatalytic degradation results of phenol solution with TiO_2 and Ag_3PO_4 catalysts. (A) phenol concentration *versus* treatment time; (B) total organic carbon concentration (TOC) *versus* treatment time. [Phenol] = 50 mg L^{-1}. O_2 bubbling flow rate: 15 L h^{-1}.

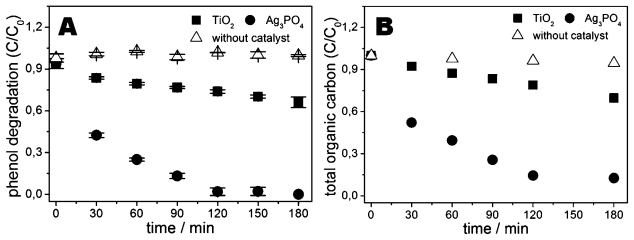

Fig. 5 Photocatalytic degradation results of phenol solution with TiO_2 and Ag_3PO_4 catalysts. (A) phenol concentration *versus* treatment time; (B) total organic carbon concentration (TOC) *versus* treatment time. [Phenol] = 50 mg L^{-1}, no O_2 bubbling.

comparison, the differences between the performances become clearer. In the present study, a simplified approach was adopted by assuming that the phenol degradation curves in Fig. 4 and 5 can be approximated by a pseudo first order reaction rate expression. Thus, the observed pseudo first-order kinetic constant, K_{obs}, were estimated. Usually in heterogeneous system K_{obs} depends on the particle surface area. Thus, values of K_{obs} were corrected for the catalysts surface area. The results are shown in Table 1. The estimated value of K_{obs} for Ag_3PO_4 is *ca.* two times larger than for TiO_2. However, when these values are corrected to take into account the particles surface area, the efficiency for Ag_3PO_4 was *ca.* 5.5 times higher than for TiO_2.

The observed behavior relative to the bubbling of oxygen in the suspension was expected for TiO_2, since it is known that molecular oxygen can improve the heterogeneous photocatalytic process, mainly for TiO_2 and related photocatalysts.[22–27] During photocatalysis, oxygen molecules often act as an electron scavenger in the electron-transfer reaction from the conductive band of the photocatalyst to oxygen, suppressing the electron–hole recombination, as described by eqn (1)–(3).

$$TiO_2 \xrightarrow{h\nu} TiO_2\left(e_{(cb)}^- + h_{(vb)}^+\right) \quad (1)$$

$$e^- + O_2 \rightarrow TiO_2 + O_2^{\bullet -} \quad (2)$$

$$h^+ + e^- \rightarrow \text{heat} \quad (3)$$

Furthermore, the superoxide anion ($O_2^{\bullet -}$) species can be formed as a consequence of the photoexcited electron trap by molecular oxygen adsorbed on the surface of TiO_2. By monitoring O_2 concentration during photocatalytic experiments it is possible to evaluate the role of O_2 molecules for both photocatalysts. Fig. 6 shows the evolution of dissolved oxygen concentration over reaction time for experiments without oxygen bubbling.

When a TiO_2 suspension without phenol was irradiated with light from the xenon lamp, O_2 concentration decreased with time, due to oxygen consumption. The decrease in O_2 concentration was much more intense when the solution contained phenol was illuminated (Fig. 6b). In this case, dissolved O_2 concentration decreased to values around 0.3 mg L^{-1} in *ca.* 40 minutes, and remained at this level. This behavior is in accordance with the previously described role of oxygen.

A different behavior was observed for dissolved oxygen in the case of Ag_3PO_4 aqueous suspension. As shown in Fig. 6, a pronounced increase in dissolved oxygen concentration was observed when the Ag_3PO_4 aqueous suspension was irradiated with the xenon lamp. In 50 minutes, dissolved oxygen concentration reached a maximum of 13.6 mg L^{-1}. In the case of Ag_3PO_4 and phenol solution, differently from TiO_2, dissolved oxygen concentration remained unchanged during the period of light irradiation, as shown in Fig. 6b.

Among the different radical species that can be formed by TiO_2 during the photocatalytic process, the hydroxyl radicals ($^{\bullet}OH$) are known to play a prominent role in organic pollutant oxidation/degradation. Thus, it is important to evaluate if $^{\bullet}OH$ radicals are produced during the Ag_3PO_4 photocatalytic process. The photooxidative properties of Ag_3PO_4 were originally discussed by Yi *et al.*[7] These authors showed results on the O_2 evolution over Ag_3PO_4 in an aqueous silver nitrate solution under visible light irradiation and studied the degradation of methylene blue. The possible reaction involved in molecular oxygen evolution from the H_2O oxidation can be represent by eqn (4).

$$H_2O_{ads} + h_{(vb)}^+ \rightarrow 1/2O_2 + 2H^+ \quad (4)$$

Indeed the reduction potential (or energy) of the valence band in Ag_3PO_4 (+2.90 V *vs.* NHE) is sufficient to oxidize the surface adsorbed H_2O to O_2 ($E^{\circ}(O_2/H_2O) = 1.23$ V).[28] Notwithstanding, the energy in the conduction band of Ag_3PO_4 (+0.45 V *vs.* NHE) is insufficient to produce oxidizing species like $O_2^{\bullet -}$ and $HO_2^{\bullet}$, since the potential needed to reduce the O_2 is "more negative" ($E^{\circ}(O_2/O_2^{\bullet -}) = -0.33$ V *vs.* NHE; $E^{\circ}(O_2/HO_2^{\bullet}) =$

Table 1 Observed values of the pseudo first-order kinetic constant, K_{obs}, for experiments on photocatalytic degradation of phenol[a]

		K_{obs} (min^{-1}) [Phenol] = 50 mg L^{-1}		K_{obs}/surface area (min^{-1} m^2 g^{-1})
	Surface area (m^2 g^{-1})	Without Oxygen	Oxygen bubbling	#K_{obs} (without O_2) *K_{obs} (O_2 bubbling)
Ag_3PO_4	18	2.7×10^{-2}	2.0×10^{-2}	#1.5×10^{-3}
TiO_2	50	1.8×10^{-3}	1.3×10^{-2}	*2.7×10^{-4}

[a] The constants were obtained for phenol degradation experiments in the following conditions: [Phenol] = 50 mg L^{-1}; 15 L h^{-1} O_2 bubbling for TiO_2; no oxygen bubbling for Ag_3PO_4.

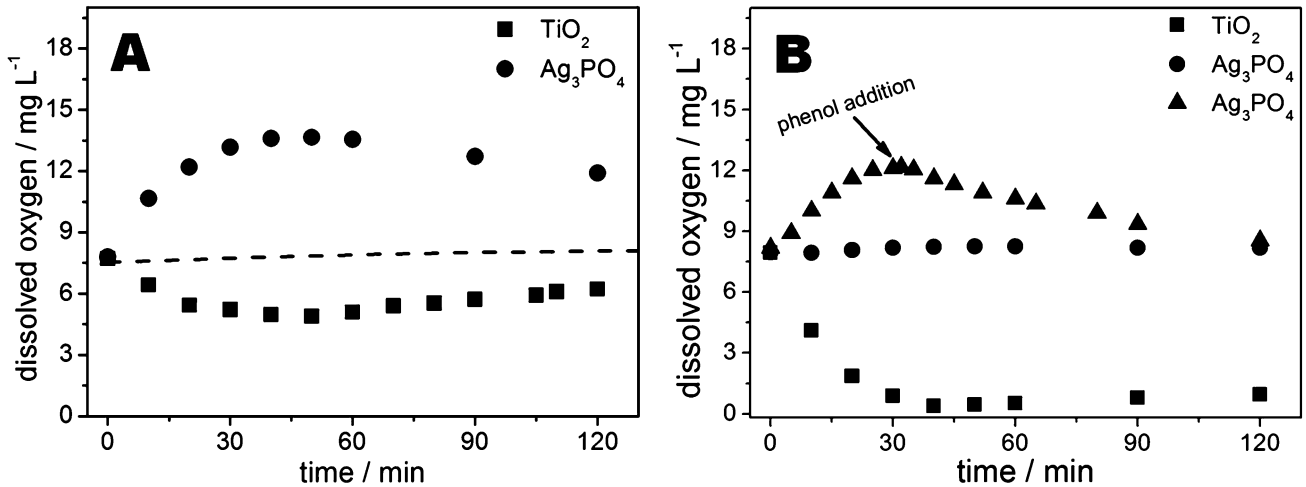

Fig. 6 Dissolved oxygen concentration over time. (A) water without phenol; (B) phenol aqueous solution. The dashed line represents dissolved oxygen concentration in H_2O under illumination by xenon lamp. [Phenol] = 50 mg L^{-1}.

−0.55 V *vs.* NHE). Fig. 7 shows the formation of hydroxyl radicals (˙OH) on the surface of both materials, TiO_2 and Ag_3PO_4, as monitored by photoluminescence using coumarin as a probe molecule.[14] The coumarin molecules can reacted with ˙OH to produce a highly fluorescent product, 7-hydroxicoumarin. Thus, PL intensity is proportional to the amount of hydroxyl radicals generated on the photocatalyst surface. As expected, for TiO_2 the generation of ˙OH was confirmed by the increase of photoluminescence intensity at about 456 nm. However, no significant changes in the PL spectra was observed when Ag_3PO_4 particles were irradiated.

Based on these results, apparently none of the hydroxyl radicals were detected during the irradiation time of Ag_3PO_4. Thus, the radical species that were possibly involved in the phenol oxidation in the photocatalytic process were probably not produced by Ag_3PO_4. However, the standard reduction potential to phenol at pH = 5.5 is $E^{\circ}_{red} = 1.14$ V, which is close to that necessary for molecular oxygen formation.[29] Therefore, phenol may have been oxidized at the surface of Ag_3PO_4 particles by the photogenerated holes (h^+). This is indicated by monitoring the dissolved oxygen concentration, as shown in Fig. 6b (triages). In this case, phenol was added to an aqueous suspension of Ag_3PO_4 particles after 30 minutes of irradiation in order to attain 50 mg L^{-1} phenol concentration. As shown in the plot, immediately after phenol addition, dissolved oxygen concentration decreased continuously during the other 60 minutes of reaction. It should be noted that oxygen evolution and phenol oxidation reaction on surface trapped holes occur competitively during photocatalysis.

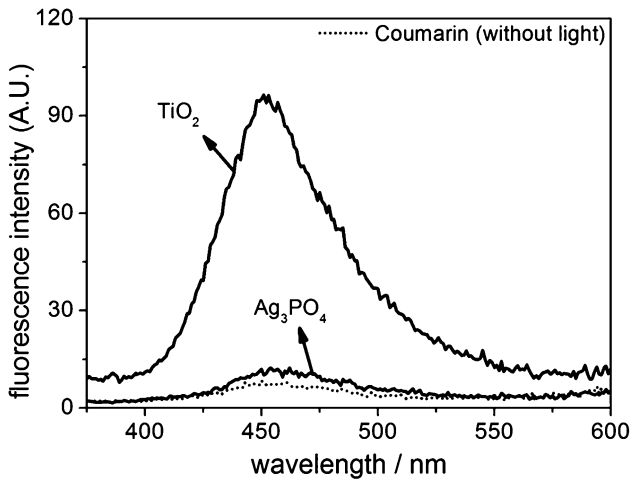

Fig. 7 Fluorescence spectra of coumarin aqueous solution after contact with TiO_2 and Ag_3PO_4 particles, under irradiation. The coumarin aqueous suspension with catalyst was irradiated for 10 minutes. Excitation wavelength: 332 nm.

Based on these experimental evidences, apparently another factor, such as charge separation, mobility, lifetime of photogenerated electrons and holes, texture or catalyst morphology may have affected the photocatalytic efficiency of catalyst particles in the phenol oxidation process. One of the possible reasons for the high oxidation efficiency of TiO_2 is its ability to inject photoexcited electrons into molecular oxygen adsorbed on the TiO_2 surface. Due to the stoichiometry of the photocatalytic reactions, h^+, or radical species produced by them, are the initiators of the phenol oxidation reactions.[23,28] As discussed before, in the case of Ag_3PO_4 photoexcited electrons cannot be consumed by oxygen. However, excited electrons have sufficient energy to reduce Ag^+ ($E^{\circ}(Ag^+/Ag^0) = +0.80$ V *vs.* NHE)) ions distributed over the sites with two-fold symmetry, which are present in Ag_3PO_4 crystalline structure. If Ag^+ ions are consumed during photoirradiation, e^-/h^+ recombination can be drastically reduced, thus increasing the probability of phenol oxidation in positive holes at the Ag_3PO_4 particle surface.

In fact, fotoexcited electron scavenged by Ag^+ ions can be observed after the photocatalytic process. Fig. 8 shows Raman spectra of Ag_3PO_4 before and after 60 minutes of light irradiation.

Pure Ag_3PO_4 shows a band at 910 cm^{-1}, which is characteristic of Ag_3PO_4 stretching.[30] After 60 minutes of light irradiation,

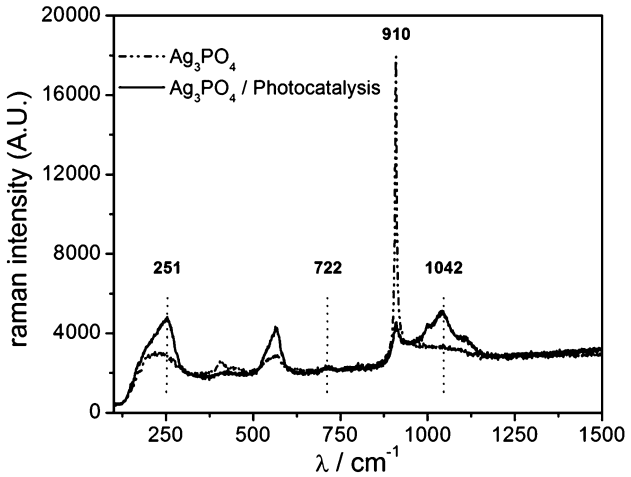

Fig. 8 Raman spectra for Ag_3PO_4 before and after the photocatalytic process.

the Raman spectrum showed vibration modes assigned to Ag_2O formation.[31] Possibly, when Ag^0 is formed the exposition to the oxidant environment leads to silver oxide. Thus, even in absence of the scavenger species, like O_2, the stoichiometry of the photocatalytic reactions is satisfied.

4. Conclusions

Silver orthophosphate (Ag_3PO_4) micrometric particles were prepared by a simple method. The photocatalytic activity of the Ag_3PO_4 was investigated relative to phenol degradation under xenon lamp irradiation. The performance in degradation of phenol in aqueous solution was compared with TiO_2 P25 photocatalyst under the same experimental conditions. Ag_3PO_4 showed a higher photocatalytic activity than TiO_2. Based on the surface area of the particles of both materials, the efficiency of Ag_3PO_4 particles was *ca.* 5.5 times higher than TiO_2. By monitoring dissolved oxygen concentration over reaction time of the photocatalytic process, important evidences were obtained relative to the reaction mechanisms when each photocatalyst is used. An explanation for the observed behavior is that there could be a competitive reaction between O_2 evolution and phenol oxidation for the positive holes on the surface of the photocatalyst particles.

The observed behavior of the Ag_3PO_4 particles relative to phenol photo oxidation opens important perspectives for the application of this material in effluent treatment, since the process is less sensitive to the presence of oxygen and can be carried out under conditions closer to visible light.

Acknowledgements

The authors would like to thank the financial support by FAPESP – São Paulo State Research Support Foundation and Brazilian Research Council (CNPq). The authors are grateful to Professor Claudio A. Oller Nascimento coordinator of the Chemical Systems Engineering Center (CESQ/DEQ-EPUSP) and Center for Environmental Research and Training (CEPEMA-USP) for the analytical facilities. The authors also thank Professor Paulo C. Isolani for the English revision.

Notes and references

1 D. T. Sawyer and J. S. Valentine, *Acc. Chem. Res.*, 1981, **14**, 393–400.
2 T. Olmez-Hanci and I. Arslan-Alaton, *Chem. Eng. J.*, 2013, **224**, 10–16.
3 P. R. Gogate and A. B. Pandit, *Adv. Environ. Res.*, 2004, **8**, 553–597.
4 P. R. Gogate and A. B. Pandit, *Adv. Environ. Res.*, 2004, **8**, 501–551.
5 U. Diebold, *Surf. Sci. Rep.*, 2003, **48**, 53–229.
6 U. I. Gaya and A. H. Abdullah, *J. Photochem. Photobiol., C*, 2008, **9**, 1–12.
7 Z. Yi, J. Ye, N. Kikugawa, T. Kako, S. Ouyang, H. Stuart-Williams, H. Yang, J. Cao, W. Luo, Z. Li, Y. Liu and R. L. Withers, *Nat. Mater.*, 2010, **9**, 559–564.
8 J. Ma, J. Zou, L. Li, C. Yao, Y. Kong, B. Cui, R. Zhu and D. Li, *Appl. Catal., B*, 2014, **144**, 36–40.
9 Y. Liu, L. Fang, H. Lu, Y. Li, C. Hu and H. Yu, *Appl. Catal., B*, 2012, **115–116**, 245–252.
10 X. Yan, Q. Gao, J. Qin, X. Yang, Y. Li and H. Tang, *Ceram. Int.*, 2013, **39**, 9715–9720.
11 B. Zheng, X. Wang, C. Liu, K. Tan, Z. Xie and L. Zheng, *J. Mater. Chem. A*, 2013, **1**, 12635–12640.
12 A. Khan, M. Qamar and M. Muneer, *Chem. Phys. Lett.*, 2012, **519–520**, 54–58.
13 S. Brunauer, P. H. Emmett and E. Teller, *J. Am. Chem. Soc.*, 1938, **60**, 309–319.
14 G. Louit, S. Foley, J. Cabillic, H. Coffigny, F. Taran, A. Valleix, J. P. Renault and S. Pin, *Radiat. Phys. Chem.*, 2005, **72**, 119–124.
15 K. S. W. Sing, D. H. Everett, R. A. Haul, W. L. Moscou, R. A. Pierotti, J. Rouquérol and T. Siemieniewska, *Pure Appl. Chem.*, 1985, **57**, 603–619.
16 H. N. Ng, C. Calvo and R. Faggiani, *Acta Crystallogr., Sect. B*, 1978, **34**, 898–899.
17 Y. M. Koshtyal, A. A. Malkov, K. L. Vasilyeva, N. V. Zakharova and A. A. Malygin, *Russ. J. Gen. Chem.*, 2013, **83**, 231–237.
18 M. A. Henderson, *Surf. Sci. Rep.*, 2011, **66**, 185–297.
19 Z.-M. Yang, G.-F. Huang, W.-Q. Huang, J.-M. Wei, X.-G. Yan, Y.-Y. Liu, C. Jiao, Z. Wan and A. Pan, *J. Mater. Chem. A*, 2014, **2**, 1750–1756.
20 A. C. S. Porfirio, J. L. De Souza, G. B. Lyra and M. A. Maringolo Lemes, *Energy*, 2012, **44**, 584–592.
21 S. X. Chu and L. H. Liu, *Sol. Energy*, 2009, **83**, 1390–1404.
22 K.-i. Okamoto, Y. Yamamoto, H. Tanaka, M. Tanaka and A. Itaya, *Bull. Chem. Soc. Jpn.*, 1985, **58**, 2015–2022.
23 B. Ohtani, *Chem. Lett.*, 2008, **37**, 13.
24 O. Legrini, E. Oliveros and A. M. Braun, *Chem. Rev.*, 1993, **93**, 671–698.
25 M. N. Chong, B. Jin, C. W. K. Chow and C. Saint, *Water Res.*, 2010, **44**, 2997–3027.

26 H. Gerischer and A. Heller, *J. Phys. Chem.*, 1991, **95**, 5261–5267.
27 K. Gopalakrishnan, H. M. Joshi, P. Kumar, L. S. Panchakarla and C. N. R. Rao, *Chem. Phys. Lett.*, 2011, **511**, 304–308.
28 X. Chen, S. Shen, L. Guo and S. S. Mao, *Chem. Rev.*, 2010, **110**, 6503–6570.
29 C. Li and M. Z. Hoffman, *J. Phys. Chem. B*, 1999, **103**, 6653–6656.
30 P. Dong, Y. Wang, B. Cao, S. Xin, L. Guo, J. Zhang and F. Li, *Appl. Catal., B*, 2013, **132–133**, 45–53.
31 M. M. Rahman, S. Bahadar Khan, A. Jamal, M. Faisal and A. M. Asiri, *Chem. Eng. J.*, 2012, **192**, 122–128.